

Systematic Structure–Property Investigations on a Series of Alternating Carbazole–Thiophene Oligomers

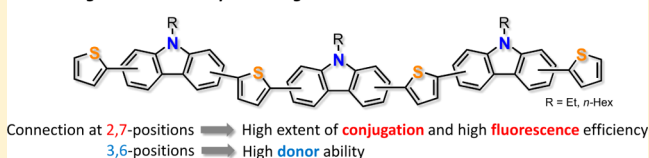
Shin-ichiro Kato, Satoru Shimizu, Atsushi Kobayashi, Toshitada Yoshihara, Seiji Tobita, and Yosuke Nakamura*

Division of Molecular Science, Faculty of Science and Technology, Gunma University, 1-5-1 Tenjin-cho, Kiryu, Gunma 376-8515, Japan

S Supporting Information

ABSTRACT: A series of alternating carbazole–thiophene oligomers, namely 2,7-linked carbazole–thiophene oligomers **1**, **3**, **5**, **7**, and **9** and 3,6-linked ones **2**, **4**, **6**, **8**, and **10**, in which the molecular length was systematically elongated, were synthesized by Suzuki–Miyaura coupling reactions. The effects of the conjugation connectivity between the carbazole and thiophene moieties and the molecular length on the electronic, photophysical, and electrochemical properties of **1**–**10** were comprehensively investigated. In the present oligomer architectures, the connection with thiophene at the 2,7-positions of carbazole ensures π -conjugation to a high extent and high fluorescence quantum yields, while that at the 3,6-positions enhances the donor ability. The increase in the molecular length of the 2,7-linked oligomers effectively extends π -conjugation. The relationship between structural variations and photophysical properties was examined by fluorescence lifetime measurements in detail. The X-ray crystal structure of **6** was also disclosed.

Alternating Carbazole–Thiophene Oligomers



INTRODUCTION

π -Conjugated oligomers and polymers have attracted much attention in recent decades due to their potential uses as semiconductors and electroactive materials in diverse organic electronic devices such as organic field-effect transistors (OFETs), organic light-emitting diodes (OLEDs), organic solar cells (OSCs), and nonlinear optical devices.^{1,2} In particular, the development of conjugated oligomers with extended π -electron delocalization is important,³ because the systematic study on monodisperse oligomers with a precisely defined length and constitution allows the elucidation of various properties, which are dependent on the molecular length and chemical structures, and sheds light on the properties of polymers.⁴ π -Conjugated oligomers have the advantage in the fine-tuning of the electronic, photophysical, and electrochemical properties by rational structural modification to achieve high device performance. Moreover, π -conjugated oligomers with sophisticated functionality are now key components in molecular electronics.⁵

Carbazole has fine optical properties, a low redox potential, and high chemical stability, and thereby oligo-/polycarbazoles have been representative benchmark materials in OFETs, OLEDs, and OSCs.^{6–8} Poly(3,6-carbazole)s and 3,6-functionalized carbazoles have been extensively studied over the past few decades, because carbazole can be easily functionalized by electrophilic substitution at its 3,6-positions (*para* positions from the nitrogen atom) with high electron density. The recent development in carbazole chemistry has also established the efficient synthetic pathways to 1,8- and 2,7-functionalized carbazoles, and their peculiar properties which are apparently different from those of 3,6-carbazole derivatives have been

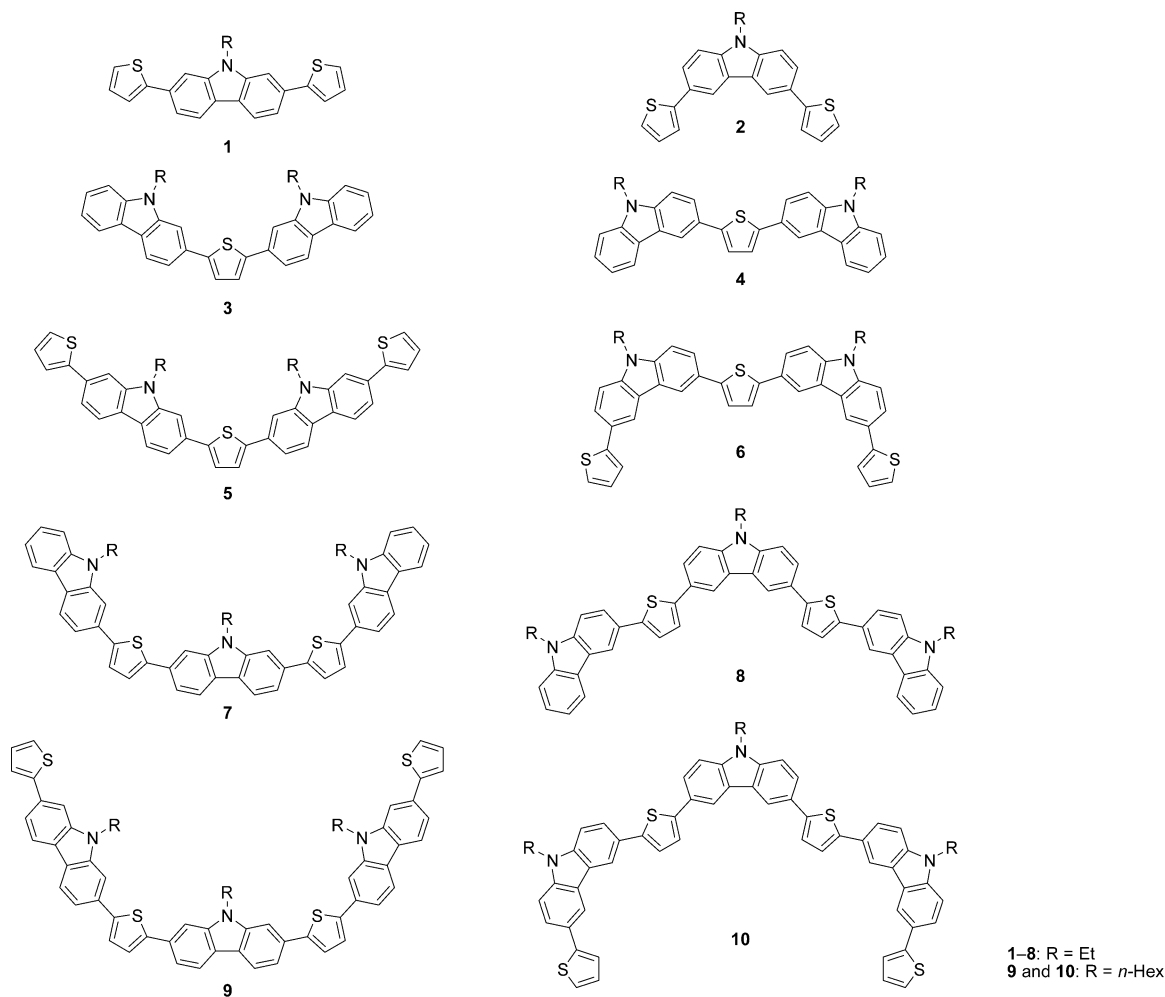
disclosed.^{6c,9,10} In this context, carbazole can be regarded as an important scaffold for the construction of π -functional materials due to its rich diversity in structural modification. Oligothiophenes, in particular, α -oligothiophenes, are among the most intensively investigated organic compounds for a variety of materials applications,¹¹ and hence mixed π -conjugated oligomers composed of carbazole and thiophene moieties have recently attracted considerable attention from the viewpoint of their potential as the active component of organic electronics and synthetic accessibility. Various carbazole–thiophene hybrid oligomers as functional materials through the use of their fluorescence and donor properties were reported;¹² in particular a large number of derivatives possessing the anchoring and acceptor group used for OSCs have been recently synthesized since the pioneering work by Koumura, Hara, and co-workers.^{13,14} However, less attention was paid to the clarification of the structure–property relationships in the carbazole–thiophene-based π -systems, which are indispensable for materials design.

We have recently synthesized a large series of thienyl-substituted carbazole derivatives (thienylcarbazoles) including **1** and **2** shown in Chart 1 and investigated the effects of the conjugation connectivity between the carbazole and thiophene moieties on the photophysical and electrochemical properties.^{8a} It was shown that **1** displays the red-shifted longest absorption maximum ($\lambda_{\text{max}}^{\text{abs}}$) and a high fluorescence quantum yield compared to **2**, while **2** has a lower oxidation potential than **1**. These findings indicate that the thienyl substituents at the 2,7-

Received: October 29, 2013

Published: December 23, 2013

Chart 1. Linear 2,7- and 3,6-Linked Carbazole–Thiophene Oligomers 1–10



positions of carbazole effectively extend π -conjugation and enhance fluorescence efficiency, while those at the 3,6-positions increase the donor ability. On the basis of this study, we became interested in the following two questions: Does the effect of the conjugation connectivity between the carbazole and thiophene moieties on the properties found in thienylcarbazole π -systems generally apply to extended π -systems, namely conjugated oligomeric structures? Does the gradual increase in the thienylcarbazole unit extend the π -conjugation and consequently enhance the fluorescence efficiency and donor potency? To approach these questions, we undertook the design and synthesis of alternating carbazole–thiophene oligomers, namely 2,7-linked carbazole–thiophene oligomers 3, 5, 7, and 9 and 3,6-linked ones 4, 6, 8, and 10 (Chart 1).¹⁵ A large series of oligomers 1–10, in which the molecular length varies systematically, allow us to study the relevant structure–property relationships in carbazole–thiophene hybrid oligomers. Herein, we report the synthesis and properties, such as the structural features and the electronic, photophysical, and electrochemical properties, of 3–10 together with 1 and 2 based on X-ray diffraction analysis, UV–vis and fluorescence spectral measurements, fluorescence lifetime measurements, cyclic voltammetry (CV), and theoretical calculations.

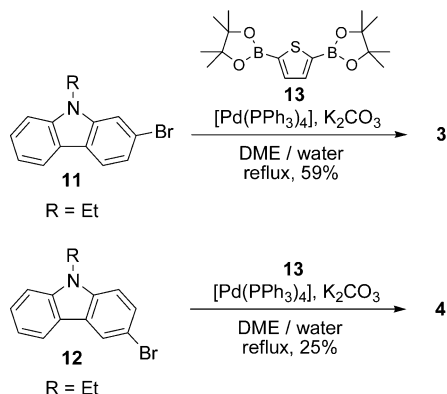
RESULTS AND DISCUSSION

Synthesis. In our molecular design, ethyl groups were introduced on the nitrogen atoms in 1–8, while the solubilizing hexyl groups were introduced in 9 and 10 to alleviate the anticipated solubility problems. Compounds 1–10 were synthesized by Suzuki–Miyaura cross-coupling reactions as key steps as described below.¹⁶ For all the reactions, $[\text{Pd}(\text{PPh}_3)_4]$ was used as the catalyst. As shown in Scheme 1, the cross-coupling reactions were performed on either bromide 11 or 12 with 2,5-bis-thiopheneboronic acid pinacol ester (13) to give 3 and 4 in 59% and 25% yields, respectively.

The syntheses of 5 and 6 were achieved by sequential Suzuki–Miyaura cross-coupling reactions from dibromides 14 and 15, respectively (Scheme 2). Thus, the reaction of 14 and 2-thiopheneboronic acid pinacol ester (16) gave monothienyl-substituted carbazole 17, which was allowed to react with 13 to furnish 5 in 33% yield. In a similar manner, 6 was prepared in two steps from 15.

The synthesis of 7 and 8 was outlined in Scheme 3. The lithium–bromine exchange between 14 and *n*-BuLi followed by the successive addition of trimethoxyborane and aqueous HCl gave diboronic acid 19, which was converted to diboronic acid pinacol ester 20 in 18% yield in two steps. Likewise, 11 was converted to boronic acid pinacol ester 22 via boronic acid 21. Bromide 24 was prepared by the coupling reaction of 22 and 3 equiv of 2,5-dibromothiophene (23) in 20% yield and then was

Scheme 1. Synthesis of 3 and 4

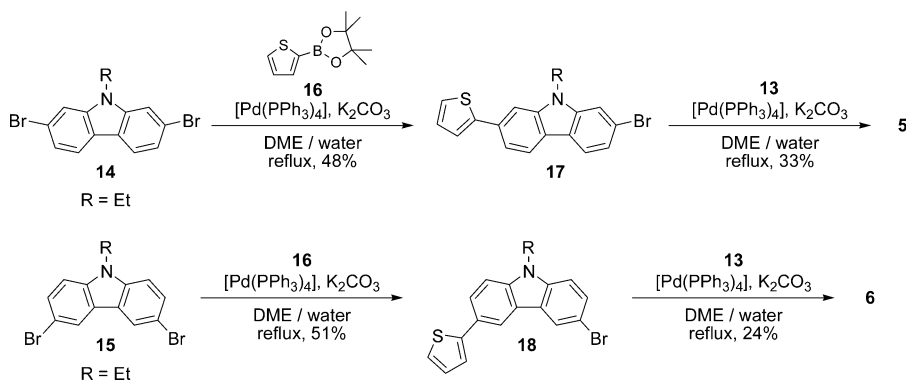


subjected to the coupling reaction with **20** to furnish **7** in 63% yield. Compound **8** was synthesized following a two-step transformation from **2**. Thus, the bromination of **2** with NBS was carried out, and then the cross-coupling reaction of dibromide **25** with **26** afforded the desired **8** in 64% yield.

The synthesis of **9** started from dibromide **27** which was allowed to react with 0.5 equiv of **16** to give **28** (Scheme 4). The transformation of a bromo group in **28** into an iodo group was performed with excess amounts of CuI/LiI in DMSO to give **29**. Subsequent cross-coupling of iodide **29** with **30** gave bromo-substituted thienylcarbazole **31**, which was further subjected to the coupling reaction with **32** to afford **9** in 24% yield. Bromination of **33** with 1 equiv of NBS afforded monobromide **34**. By the cross-coupling reaction of **34** with **35**, compound **10** which was the final member of this series of oligomers was obtained in 23% yield. All the compounds were fully characterized by various spectroscopic methods, such as $^1\text{H NMR}$, $^{13}\text{C NMR}$, and mass spectroscopy and/or elemental analysis.

Crystal Structure of 6. The single crystal of **6** suitable for X-ray diffraction analysis was obtained by vapor diffusion of hexane into CH_2Cl_2 solution (Figure 1a,b). The molecule adopts an all *s*-trans conformation between the carbazole and thiophene moieties.¹⁷ The solid-state structure of **6** is quasi-planar with torsion angles between the carbazole and thiophene moieties of 9.0° – 19.7° . Compound **6** forms the stacked dimer structure by effective π – π interactions, and the dimer is again packed in a herringbone fashion by CH – π interactions; no noticeable π – π interaction is observed between the neighboring dimers (Figure S1 in the Supporting Information).

Scheme 2. Synthesis of 5 and 6



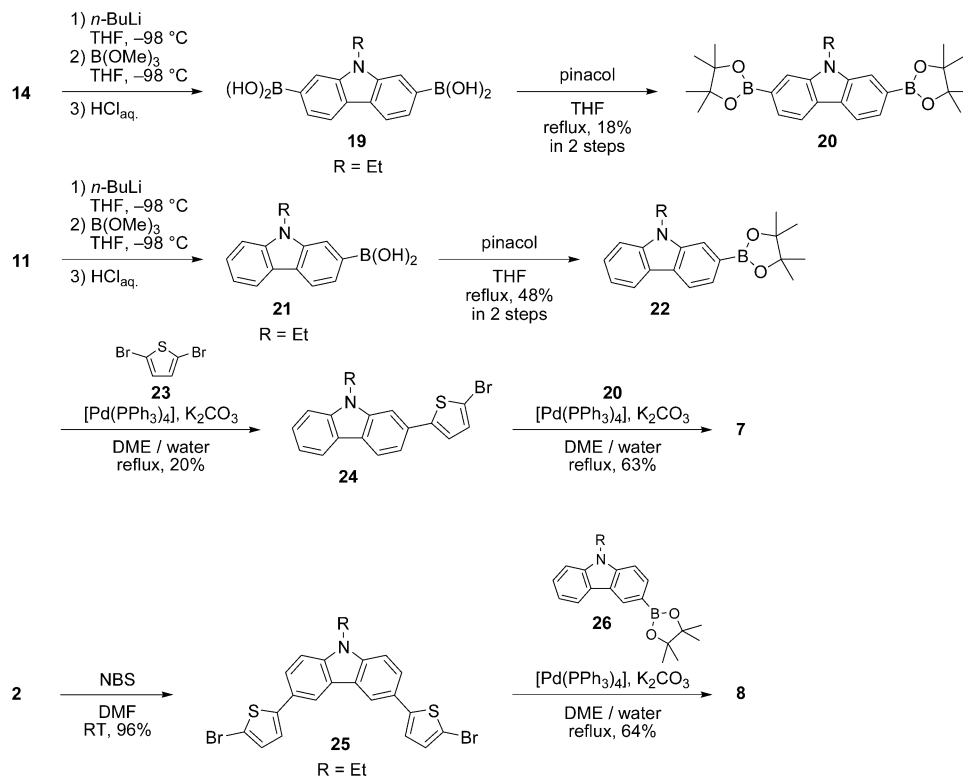
To gain insight into the molecular structure of **6**, we optimized the ground-state structure of **6'**, in which the ethyl groups in **6** were replaced with the methyl groups, by density functional theory (DFT) calculations at the B3LYP/6-31G(d) level of theory by the Gaussian 09 program.^{18,19} The selected geometrical parameters of **6'** are given in Table S1 in the Supporting Information and compared with the crystallographic dihedral angles and bond lengths for **6**. As for the bond lengths, there is good agreement between the experiment and theory in general. The differences in carbon–carbon bond lengths and carbon–nitrogen bond lengths are within 0.026 Å. The large deviation occurs for the carbon–sulfur bond lengths, with the DFT results providing longer bond lengths of 0.025–0.046 Å than the X-ray results. The dihedral angles between the carbazole and thiophene moieties are calculated to be 27° – 29° , and hence the DFT results provided larger angles than those in the X-ray results by *ca.* 10° – 15° . This finding implies the contribution of the crystal packing force to the observed high planarity of **6** in the solid state.²⁰

Electronic Absorption Spectroscopy. We measured the UV–vis absorption spectra of oligomers **1**–**10** in CH_2Cl_2 solutions (Figure 2a,b), and the $\lambda_{\text{max}}^{\text{abs}}$ values for discussion on the extension of π -conjugation are summarized in Table 1. As expected from our recent finding that the longest $\lambda_{\text{max}}^{\text{abs}}$ value of **1** (353 nm) is red-shifted relative to that of **2** (314 nm), the longest $\lambda_{\text{max}}^{\text{abs}}$ values of 2,7-linked carbazole–thiophene oligomers **3**, **5**, **7**, and **9** are apparently red-shifted as compared to those of the corresponding 3,6-linked oligomers **4**, **6**, **8**, and **10**. Thus, it can be reasonably concluded that the connection with thiophene at the 2,7-positions of carbazole in general extends π -conjugation effectively relative to that at the 3,6-positions in the oligomer architectures. Noticeably, the molar extinction coefficients (ϵ) at the longest $\lambda_{\text{max}}^{\text{abs}}$ of 2,7-linked oligomers **1**, **3**, **5**, **7**, and **9** are larger than those of the corresponding 3,6-linked oligomers **2**, **4**, **6**, **8**, and **10**.

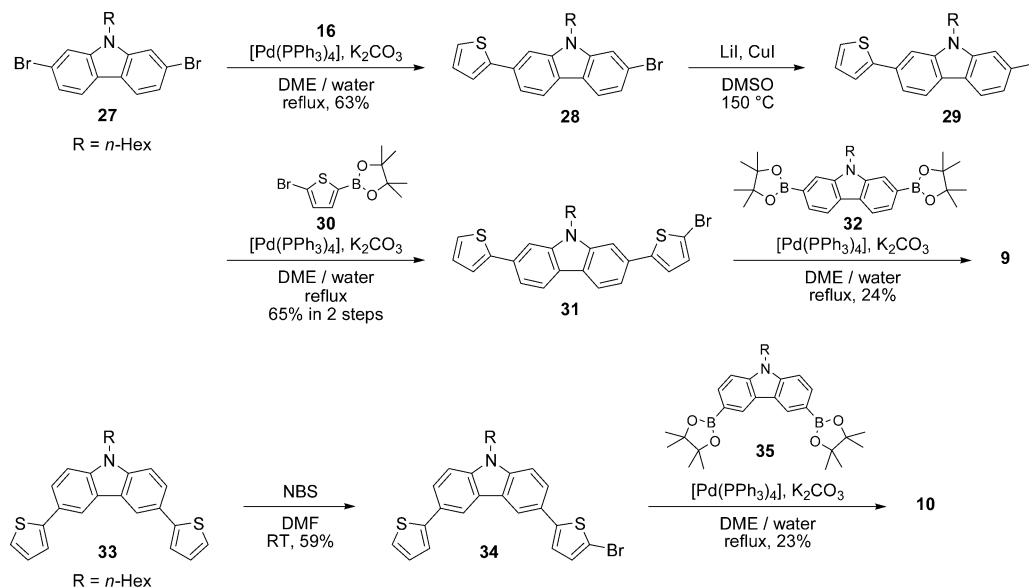
In the series of the 2,7-linked oligomers, clear red shifts of the longest $\lambda_{\text{max}}^{\text{abs}}$ values were observed from **1**, **3**, **5**, **7**, to **9**, indicative of the effective extension of π -conjugation upon increasing the molecular length (Figure 2a). It seems that **9** does not reach the effective conjugation length for this system and longer oligomers exhibit further red-shifted longest $\lambda_{\text{max}}^{\text{abs}}$ values. Oligomers **1**, **3**, **5**, **7**, and **9** feature similar absorption curves to each other in the low-energy region, and their ϵ values at the $\lambda_{\text{max}}^{\text{abs}}$ steadily increase with the number of heteroaromatic rings.

In sharp contrast to the series of oligomers **1**, **3**, **5**, **7**, and **9**, no pronounced red shift of the longest $\lambda_{\text{max}}^{\text{abs}}$ values was

Scheme 3. Synthesis of 7 and 8



Scheme 4. Synthesis of 9 and 10



observed in the series of 3,6-linked oligomers 2, 4, 6, 8, and 10 upon increasing the molecular length (Figure 2b). For example, the terminal thienyl functionality in 6 and 10 results in the marginal or almost no red shift of the longest $\lambda_{\text{max}}^{\text{abs}}$ values as compared to those of 4 and 8, respectively (354 nm (4), 362 nm (6), 380 nm (8), 380 nm (10)). The spectral change and the red shift of the absorption band in the low-energy region were hardly observed with increase in the molecular length by reversing the thiophene and carbazole moieties from 6 to 8, whereas the significant spectral change and the clear red shift of the absorption onset were observed from 2 to 4. These findings suggest that 3,6-linked carbazole–thiophene oligomers 4, 6, 8,

and 10 possess almost the same effective conjugation length and/or the increase in the molecular length in this series decreases the planarity of the π -conjugated backbone as predicted by theoretical calculations (*vide infra*).²¹

Fluorescence Spectroscopy. All of the carbazole–thiophene oligomers 1–10 are fluorescent. The fluorescence spectra of 2,7-linked oligomers 1, 3, 5, 7, and 9 and 3,6-linked ones 2, 4, 6, 8, and 10 in CH₂Cl₂ (10⁻⁵–10⁻⁶ mol L⁻¹) are shown in Figure 3a and 3b, respectively, and the spectral data are summarized in Table 2.²² The color of the fluorescence of 1–10 ranges from violet, blue, to light green. The two well-defined vibronic maxima were observed in the fluorescence

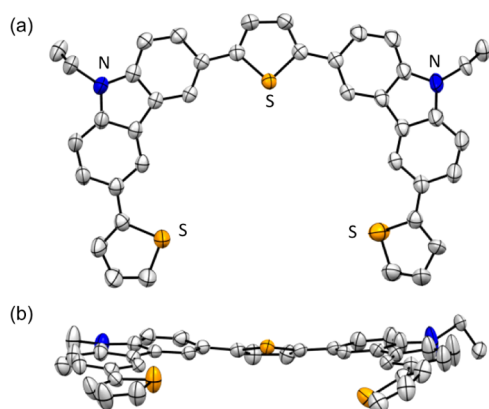


Figure 1. X-ray crystal structure of **6**. (a) Top view and (b) side view. Displacement ellipsoids are shown at the 50% probability level. Hydrogen atoms are omitted for clarity.

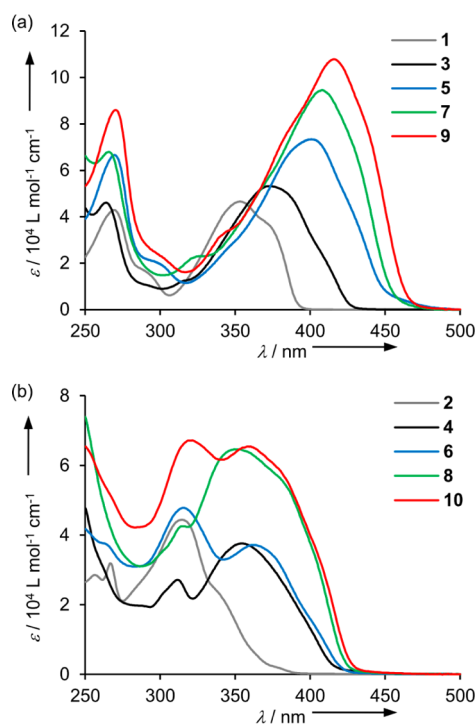


Figure 2. Electronic absorption spectra of (a) **1**, **3**, **5**, **7**, and **9** and (b) **2**, **4**, **6**, **8**, and **10** in CH_2Cl_2 at 298 K.

spectra of **1–10**. The fluorescence spectra of 2,7-linked oligomers **1**, **3**, **5**, **7**, and **9** do not seem to be the mirror image of the absorption spectra. The broad absorption band in the low energy region and the vibronic fine structure in the fluorescence spectra of **1**, **3**, **5**, **7**, and **9** suggest the contribution of a more rigid structure in the excited state, namely the quinoid state, than the ground state.²³ The fluorescence maxima ($\lambda_{\text{max}}^{\text{fl}}$) of the series of **1**, **3**, **5**, **7**, and **9** are gradually red-shifted upon increasing the molecular length. Similar to the change of the longest $\lambda_{\text{max}}^{\text{abs}}$ values, the red shift of the $\lambda_{\text{max}}^{\text{fl}}$ values from **1** to **9** is noticeably large as compared to that from **2** to **10** (391 nm (**1**), 392 nm (**2**), 464 nm (**9**), 429 nm (**10**)). The Stokes shifts for **2**, **4**, **6**, **8**, and **10** are essentially larger than those for the corresponding **1**, **3**, **5**, **7**, and **9**, indicating a somewhat large structural change and/or electronic distribution change, which should facilitate the nonradiative process, in the former rather than the latter.

Table 1. UV–vis Spectroscopic Data and Calculated Lowest Excitation Energies of **1–10**^{a,b}

	$\lambda_{\text{max}}^{\text{abs}}$ [nm]	calcd $\lambda_{\text{max}}^{\text{exc}}$ [nm] (f) ^b	composition of band ^b
1	269, 290, ^c 353	352 (1.114)	H → L, 97%
2	256, 267, 314	328 (0.336)	H – 1 → L, 8%; H → L + 1, 90%
3	264, 372	375 (1.597)	H → L, 99%
4	311, 354	359 (0.792)	H → L, 95%; H → L + 2, 2%
5	269, 401	411 (2.366)	H → L, 98%
6	315, 362	373 (0.814)	H – 1 → L + 3, 2%; H → L, 96%
7	265, 325, ^c 407	421 (2.760)	H – 1 → L + 1, 2%; H → L, 96%
8	314, 349, 380 ^c	384 (0.584)	H – 1 → L + 1, 3%; H → L, 94%
9	270, 340, ^c 416	– ^d	– ^d
10	321, 358, 380 ^c	– ^d	– ^d

^aMeasured in CH_2Cl_2 . ^bTD-DFT (TD/B3LYP/6-31G(d)) calculations were carried out with the use of optimized structures of **1'–8'**, where the Et groups in **1–8** were replaced with the Me groups, at the B3LYP/6-31G(d) level of theory; H = HOMO, L = LUMO. ^cPeak as shoulder. ^dNot calculated due to the large molecular size.

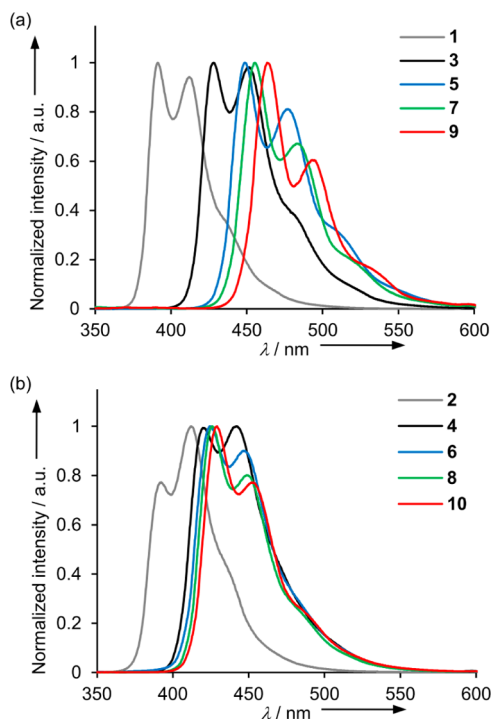


Figure 3. Fluorescence spectra of (a) **1**, **3**, **5**, **7**, and **9** and (b) **2**, **4**, **6**, **8**, and **10** on 300-nm excitation in CH_2Cl_2 at 298 K.

We determined the absolute fluorescence quantum yields (Φ_f) of **1–10** by using an integrating sphere system (Table 2). The 2,7-linked oligomers **1**, **3**, **5**, **7**, and **9** display moderate to high Φ_f values of 0.44–0.74. It is remarkable that **7** and **9** with the extensively long π -conjugated backbone display high Φ_f values of 0.74 and 0.68, respectively. Thus, they are good emitters due to a combination of high Φ_f and large ϵ values. In the series of 3,6-linked oligomers, compound **2** exhibits an exceptionally low Φ_f value of 0.036. Compounds **4** and **6** show high Φ_f values of 0.78 and 0.67, respectively. The Φ_f values of **8**

Table 2. Summary of Fluorescence Data of 1–10^a

	$\lambda_{\max}^{\text{fl}}$ [nm]	Stokes shifts [cm ⁻¹]	Φ_f^b	τ_f [ns] ^c	k_r [10 ⁷ s ⁻¹] ^d	k_{nr} [10 ⁷ s ⁻¹] ^e
1	391, 412	2750	0.44 (0.61)	2.12	20.8	26.4
2	392, 411	6330	0.036 (0.06)	1.68	2.1	57.4
3	428, 451	3510	0.50 (0.79)	0.62	80.6	80.7
4	420, 442	4430	0.78 (0.59)	0.61	128	36.1
5	448, 476	2610	0.63 (0.63)	0.74	85.1	50.0
6	424, 446	4040	0.67 (0.55)	0.64	104	51.6
7	455, 483	2530	0.74 (0.67)	0.80	92.5	32.5
8	426, 448	2840	0.33 (0.24)	0.70	47.1	95.7
9	464, 493	2540	0.68 (-) ^f	0.72	94.4	44.4
10	429, 451	3000	0.30 (0.25)	0.72	41.7	97.2

^aMeasured in CH₂Cl₂. ^bAbsolute quantum yields determined by an integrating sphere system. The values in parentheses are in cyclohexane. ^cLifetime. ^dRadiative decay constant. ^eNonradiative decay constant. ^fNot determined due to insolubility.

Table 3. Oxidation Potential (E_{pa}) and Onset (E_{onset}) by Cyclic Voltammetry in CH₂Cl₂ (0.1 mol L⁻¹ *n*-Bu₄NPF₆),^a Theoretically Calculated HOMO and LUMO Levels and Their Gaps ($\Delta E_{\text{HOMO-LUMO}}$),^b and Optical HOMO–LUMO Gaps (ΔE_{opt})^c

	E_{pa} [V]	E_{onset} [V]	HOMO ^{b,d} [eV]	LUMO ^b [eV]	$\Delta E_{\text{HOMO-LUMO}}$ ^b [eV]	ΔE_{opt} [eV]
1	+0.65 ^f	+0.55	-5.44 (-5.35)	-1.66	3.78	3.51
2	+0.54 ^f	+0.43	-5.31 (-5.23)	-1.21	4.09	3.94
3	+0.57 ^e	+0.42	-5.26 (-5.22)	-1.65	3.61	3.33
4	+0.30 ^e	+0.20	-5.02 (-5.00)	-1.20	3.82	3.50
5	+0.38 ^f	+0.31	-5.21 (-5.11)	-1.88	3.33	3.09
6	+0.30 ^e	+0.22	-5.02 (-5.02)	-1.30	3.72	3.42
7	+0.34 ^f	+0.29	-5.13 (-5.09)	-1.86	3.27	3.05
8	+0.22 ^f	+0.18	-4.91 (-4.98)	-1.26	3.65	3.55
9	+0.35 ^f	+0.30	-5.12 (-5.10)	-1.96	3.16	2.98
10	+0.25 ^e	+0.19	-4.92 (-4.99)	-1.30	3.62	3.46

^aAll potentials are given versus the Fc⁺/Fc couple used as the external standard; scan rate = 100 mV s⁻¹. ^bCalculated by B3LYP/6-31G(d,p)//B3LYP/6-31G(d) for 1'–10', where the alkyl groups on the nitrogen atoms in 1–10 are replaced with the methyl groups. ^cThe values are obtained from the longest $\lambda_{\max}^{\text{abs}}$. ^dThe values in the parentheses are those deduced from the E_{onset} values according to the following equation: HOMO = -(4.8 + E_{onset}) eV (ref 25). ^eReversible wave. ^fIrreversible wave.

(0.33) and 10 (0.30) are almost half of those of 4 and 6, and thus the Φ_f values of the 3,6-linked oligomers tend to decrease with the increase from the two to three carbazole moieties, which contrasts with the trend for the Φ_f values in the 2,7-linked oligomers. Overall, it is likely that the connection with thiophene at the 2,7-positions of carbazole ensures high fluorescence efficiency relative to that at the 3,6-positions.

To obtain further insight into the photophysical properties of 1–10, we determined the fluorescence lifetimes (τ_f) with the time-correlated single-photon counting method (Figures S3–S12)²⁴ and calculated the radiative (k_r) and nonradiative (k_{nr}) decay rate constants from the singlet excited state, based on the equations $k_r = \Phi_f/\tau_f$ and $k_{\text{nr}} = (1 - \Phi_f)/\tau_f$. Compounds 1 and 2 with the one carbazole moiety exhibit τ_f values of 2.12 and 1.68 ns, respectively. Compounds 3–10 with the two or three carbazole moieties display shorter τ_f values of 0.61–0.80 ns than 1 and 2.

Interestingly, the calculated k_r and k_{nr} values of 1–10 were found to be highly dependent on the conjugation connectivity between the thiophene and carbazole moieties and the molecular length. With increasing molecular length in the series of 2,7-linked oligomers 1, 3, 5, 7, and 9, the k_r values increase exclusively, and the increase in the k_r values from 1 to 3 is particularly remarkable (20.8×10^7 s⁻¹ (1), 80.6×10^7 s⁻¹

(3)). The clear decrease in the k_{nr} values is again observable from 3 and 5 to 7 and 9, although 1 shows the smallest k_{nr} value. Thus, the marked high Φ_f values of 5, 7, and 9 derive from a combination of the promotion of the radiative process and suppression of the nonradiative one by increasing the molecular length. In the series of 3,6-linked oligomers, compound 2 displays an exceptionally small k_r value of 2.1×10^7 s⁻¹ (*vide infra*), while 4 shows a large k_r value of 128×10^7 s⁻¹. Upon an increase in the molecular length from 4, 6, 8 to 10, the k_r values decrease and the k_{nr} values increase, which stands in sharp contrast to the trend for the values in the 2,7-linked oligomers. In particular, increasing the number of carbazole units from 4 and 6 to 8 and 10, that is, from the two to three units, drastically changes the k_r and k_{nr} values. As a consequence, the k_{nr} values are larger than the k_r values in 8 and 10, and hence the nonradiative processes become preferable to the radiative ones.

Electrochemistry. In order to elucidate the effects of the conjugation connectivity between the carbazole and thiophene units and the elongation of the molecular length on the donor ability and the electrochemical stability, we performed the CV for 1–10 in CH₂Cl₂ containing 0.1 mol L⁻¹ *n*-Bu₄NPF₆ as a supporting electrolyte (Figure S13 in the Supporting Information). The oxidation potentials (E_{pa}) and onsets (E_{onset})

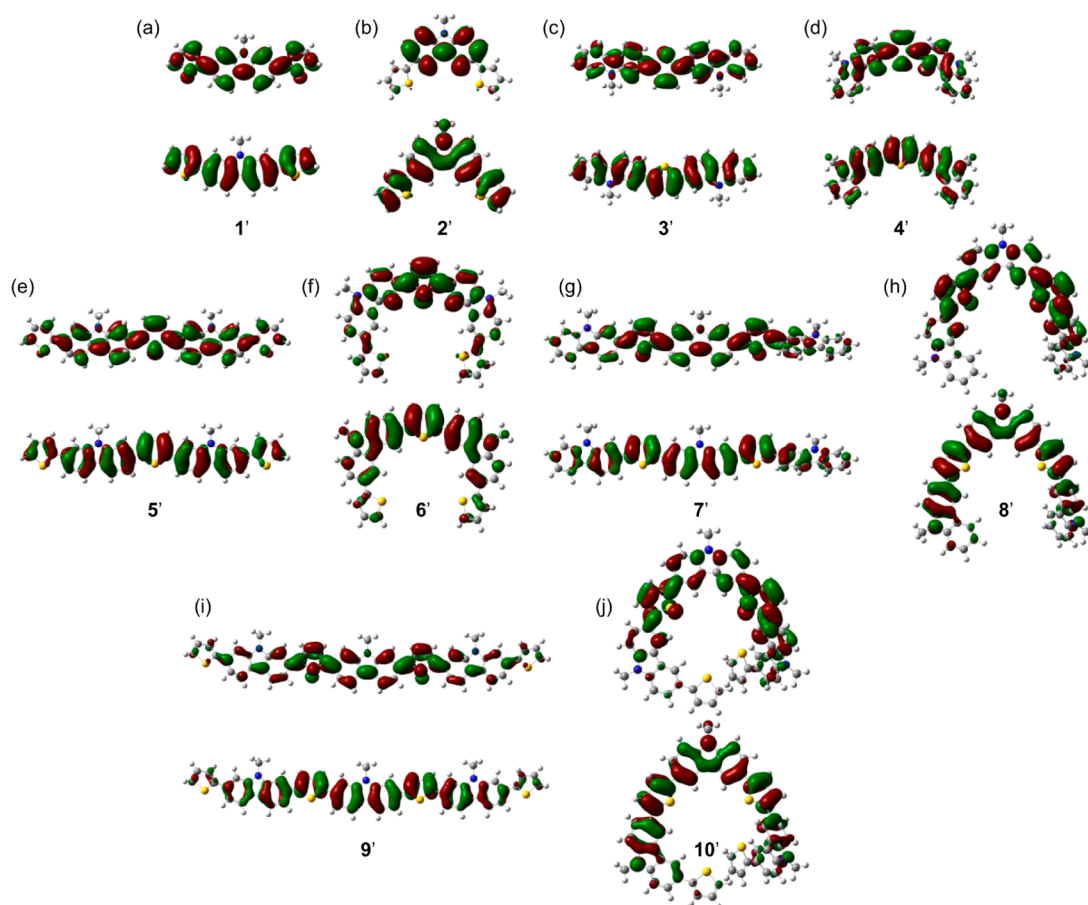


Figure 4. Molecular orbital plots (B3LYP/6-311G(d,p)//B3LYP/6-31G(d)) of (a) 1', (b) 2', (c) 3', (d) 4', (e) 5', (f) 6', (g) 7', (h) 8', (i) 9', and (j) 10'. The lower plots represent the HOMOs, and the upper plots represent the LUMOs.

versus Fc^+/Fc (ferrocenium/ferrocene couple) are listed in Table 3.

As described above, we have recently found that the thienyl functionalization at the 3,6-positions of carbazole enhances the donor ability of the resulting molecules as compared to that at the 2,7-positions. As a typical example, **2** is oxidized at a lower potential than **1**. This finding is reasonably explained by the substitution pattern of the carbazole moiety. The thienyl substituents in **1** are located at the *meta* positions relative to the nitrogen atoms of the carbazole moiety, while those in **2** are at the *para* positions. Noticeably, the effect of the conjugation connectivity on the donor ability is clearly observable in **3–10**. The first E_{pa} and E_{onset} values for 3,6-linked oligomers **4**, **6**, **8**, and **10** are cathodically shifted as compared to those for the corresponding 2,7-linked oligomers **3**, **5**, **7**, and **9**, thus demonstrating that the connection with thiophene at the 3,6-positions of carbazole effectively enhances the donor ability relative to that at the 2,7-positions in the present oligomer architectures. From **1**, **3**, **5** to **7**, the oxidations occur at potentials cathodically shifted by *ca.* 300 mV. Similarly, the oxidations are facilitated from **2**, **4**, and **6** to **8**. These results indicate that the increase in the molecular length is substantially effective for the enhancement of the donor ability. However, compounds **4** and **6**, **7** and **9**, or **8** and **10** do not differ much in the first E_{pa} and E_{onset} values, suggesting that the terminal thiophene units in **6**, **9**, and **10** make almost no contribution to the enhancement of the donor ability, which is further supported by the calculations (*vide infra*).

Oligomers **3**, **6**, and **10** displayed the reversible first oxidation waves, and **4** experienced the two reversible oxidation waves (Figure S13e). The irreversible oxidation behavior and/or the substantial peak amplitude were observed for **1**, **2**, **5**, **7**, **8**, and **9**, indicative of the instability of the cationic species. As a whole, it seems that the connection with thiophene at the 3,6-positions of carbazole brings about high electrochemical stability relative to that at the 2,7-positions, which should result from the effective resonance stabilization of the cationic species,²⁶ in addition to high donor ability.

Theoretical Calculations. To obtain further insight into the electronic properties of **1–10**, we performed the geometrical optimization and frontier molecular orbital (FMO) calculations of **1'–10'**, where the ethyl or hexyl groups of **1–10** are replaced with the methyl groups. The FMO plots and the HOMO and LUMO levels were obtained by the single-point calculations at the B3LYP/6-311G(d,p)//B3LYP/6-31G(d) level of theory. The results are summarized in Table 3, and the HOMOs and LUMOs of **1'–10'** are shown in Figure 4. The geometrical optimization suggests that the conjugated backbone of 3,6-linked oligomers **8'** and **10'** presents a deviation from planarity, while that of 2,7-linked ones **7'** and **9'** shows high planarity (Figures S15 and S16).²⁷ This may be one of the reasons for the lower extent of π -conjugation of **8** and **10** than **7** and **9**, respectively, as found in the UV–vis spectra. All the HOMOs and LUMOs are roughly delocalized over the whole π -skeleton; however, both of them seem to become gradually localized at the central part of the molecules upon an increase in the molecular length.

The calculated HOMO energy levels of 1'–10' are in good agreement with those deduced from the E_{onset} values of 1–10 within the range of ± 0.1 eV (Table 3). The calculated HOMO levels of 2', 4', 6', 8', and 10' are higher than those of the corresponding 1', 3', 5', 7', and 9', which agrees well with the finding that 3,6-linked oligomers 2, 4, 6, 8, and 10 exclusively display lower first E_{pa} and E_{onset} values than 2,7-linked ones 1, 3, 5, 7, and 9, respectively. The enhancement of the donor ability by the connection with thiophene at the 3,6-positions of carbazole relative to that at the 2,7-positions is readily interpreted as the HOMO densities. Thus, the HOMO densities of 2', 4', 6', 8', and 10' have a large contribution from the electron-rich nitrogen atoms of carbazole, whereas those of 1', 3', 5', 7', and 9' are not found on the nitrogen atoms. An increase in the molecular length from 1', 3', 5' to 7' and 9' raises the HOMO levels, as does that from 2', 4', and 6' to 8' and 10'. The HOMO levels of 6', 9', and 10' are almost the same as those of 4', 7', and 8', respectively, suggesting that the terminal thiophene moieties in 6', 9', and 10' have a marginal contribution to their HOMO densities. These findings agree well with the results in the CV. It is interesting to note that the terminal thienyl functionalization in 5', 6', 9', and 10' results in the lowering of the LUMO levels rather than the elevation of HOMO levels.

We carried out the time-dependent (TD) DFT calculations for 1'–8' to study the electronic transitions of 1–8 (Tables S2–S9); the large molecular size of 9' and 10' prevented us from performing the TD-DFT study. The results for absorption maxima of 1'–8' at the TD/B3LYP/6-31G(d)//B3LYP/6-31G(d) level of theory are summarized in Table 1. The absorption maxima in the low-energy region of 1' and 3'–8' are mainly attributed to the HOMO–LUMO transitions. On the other hand, the absorption maximum of 2' is related to the mixed HOMO–1–LUMO and HOMO–LUMO+1 transitions; thus, it is considered that the absorption tail around 380 nm of 2 is ascribed to the forbidden HOMO–LUMO transition, which may be one of the reasons for its small k_f and low Φ_f values (*vide supra*).²⁸ The calculated HOMO–LUMO gaps ($\Delta E_{\text{HOMO–LUMO}}$) are approximately comparable to the optical HOMO–LUMO gaps (ΔE_{opt}) estimated from the UV–vis spectra (Table 3). The calculations qualitatively reproduce the findings that the $\Delta E_{\text{HOMO–LUMO}}$ values become smaller upon increasing the molecular length in 2,7-linked oligomers 1', 3', 5', 7', and 9' and 3,6-linked oligomers 2', 4', 6', 8', and 10' and the change in the $\Delta E_{\text{HOMO–LUMO}}$ values in the former is significantly larger than that in the latter (3.78 eV (1'), 4.09 eV (2'), 3.16 eV (9'), 3.62 eV (10')).

CONCLUSION

We have synthesized a series of structurally well-defined, alternating carbazole–thiophene oligomers 1–10 systematically by means of Suzuki–Miyaura cross-coupling reactions as key steps. By comparing the electronic, photophysical, and electrochemical properties between 2,7-linked oligomers 1, 3, 5, 7, and 9 and 3,6-linked oligomers 2, 4, 6, 8, and 10, we have demonstrated the particular importance of the conjugation connectivity between the carbazole and thiophene moieties and the elongation of molecular length in their properties. It was found that the connection with thiophene at the 2,7-positions of carbazole causes a high extent of conjugation and high fluorescence efficiency, while that at the 3,6-positions enhances the donor ability. It is worth mentioning that our initial findings about the dependence of the properties on the conjugation

connectivity between the carbazole and thiophene moieties in thienylcarbazole derivatives are also generally applicable to the oligomer architectures. In contrast to the 3,6-linked oligomers, the increase in the molecular length of the 2,7-linked oligomers extends π -conjugation effectively and increases radiative decay constants. The experimentally obtained structure–property relationships are in qualitative agreement with the findings obtained by DFT calculations. We believe that the present study provides valuable information for the design of new carbazole–thiophene-based π -functional oligomers.

EXPERIMENTAL SECTION

General Suzuki–Miyaura Cross-Coupling Procedure for Preparation of Carbazole–Thiophene Oligomers. A mixture of haloarene (1 equiv) and K_2CO_3 (1–2 equiv) in DME/water (10:1, ~ 0.2 mol L^{-1}) was bubbled with argon with stirring for 30 min. $[\text{Pd}(\text{PPh}_3)_4]$ (ca. 2–3%, per reaction point) and boronic acid pinacol ester were added to the mixture, and the resulting mixture was refluxed under an argon atmosphere. The organic phase was separated, and the aqueous phase was extracted with toluene, CH_2Cl_2 , THF, or CHCl_3 . The combined organic phase was washed with water, dried over anhydrous MgSO_4 , and concentrated under reduced pressure. The residue was purified by column chromatography. An analytically pure material was obtained by recycling GPC eluting with CHCl_3 and/or recrystallization.

Preparation of 3. Compound 11 (0.10 g, 3.65 mmol) was allowed to react with 13 (37 mg, 0.109 mmol) in the presence of K_2CO_3 (0.10 g, 0.729 mmol) and $[\text{Pd}(\text{PPh}_3)_4]$ (25 mg, 21.9 μmol) for 15 h according to the general Suzuki–Miyaura cross-coupling procedure. The crude material was purified by column chromatography (SiO_2 , toluene/hexane = 1:3) to give 3 (30 mg, 59%) as yellow solids. Mp 233–234 °C; $^1\text{H NMR}$ (300 MHz, CDCl_3): δ 8.11 (2H, d, $J = 8.0$ Hz), 8.10 (2H, d, $J = 7.7$ Hz), 7.67 (2H, d, $J = 1.4$ Hz), 7.58 (2H, dd, $J = 8.0$ and 1.4 Hz), 7.46–7.49 (2H, m), 7.46 (2H, s), 7.41–7.44 (2H, m), 7.26 (2H, d, $J = 7.7$ Hz), 4.45 (4H, q, $J = 7.2$ Hz), 1.52 (6H, t, $J = 7.2$ Hz); $^{13}\text{C NMR}$ (150 MHz, CDCl_3): δ 140.71, 140.69, 140.5, 132.2, 125.8, 124.1, 122.9, 122.6, 120.9, 120.5, 119.2, 117.3, 108.6, 105.4, 37.7, 14.0; UV–vis (CH_2Cl_2): $\lambda_{\text{max}}^{\text{abs}}$ (ϵ) 264 (46 100), 372 (53200) nm; HR-FAB-MS (NBA, positive): m/z calcd for $\text{C}_{32}\text{H}_{26}\text{N}_2\text{S}^+$ 470.1817, found 470.1814 (M^+).

Preparation of 4. Compound 12 (0.10 g, 3.65 mmol) was allowed to react with 13 (37 mg, 0.109 mmol) in the presence of K_2CO_3 (0.10 g, 0.729 mmol) and $[\text{Pd}(\text{PPh}_3)_4]$ (25 mg, 21.9 μmol) for 15 h according to the general Suzuki–Miyaura cross-coupling procedure. The crude material was purified by column chromatography (SiO_2 , toluene/hexane = 1:3) to give 4 (13 mg, 25%) as yellow solids. Mp 183–185 °C; $^1\text{H NMR}$ (300 MHz, CDCl_3): δ 8.38 (2H, s), 8.17 (2H, d, $J = 7.8$ Hz), 7.80 (2H, d, $J = 7.7$ Hz), 7.48–7.52 (2H, m), 7.42–7.45 (2H, m), 7.42–7.44 (2H, m), 7.36 (2H, s), 7.28 (2H, d, $J = 7.8$ Hz), 4.40 (4H, q, $J = 7.2$ Hz), 1.47 (6H, t, $J = 7.2$ Hz); $^{13}\text{C NMR}$ (125 MHz, CDCl_3): δ 140.4, 139.4, 126.01, 125.90, 123.9, 123.4, 122.98, 122.95, 120.7, 119.1, 117.4, 108.84, 108.79, 108.74, 37.6, 13.9; UV–vis (CH_2Cl_2): λ_{max} (ϵ) 311 (27 100), 354 (37 600) nm; HR-FAB-MS (NBA, Positive): m/z calcd for $\text{C}_{32}\text{H}_{26}\text{N}_2\text{S}^+$ 470.1817, found 470.1783 (M^+).

Preparation of 17. Compound 14 (1.1 g, 3.09 mmol) was allowed to react with 16 (0.50 g, 2.38 mmol) in the presence of K_2CO_3 (0.66 g, 4.76 mmol) and $[\text{Pd}(\text{PPh}_3)_4]$ (82 mg, 71.4 μmol) for 15 h according to the general Suzuki–Miyaura cross-coupling procedure. The crude material was purified by column chromatography (SiO_2 , toluene/hexane = 1:5) to give 17 (0.41 g, 48%) as pale yellow solids. Mp 130–132 °C; $^1\text{H NMR}$ (300 MHz, CDCl_3): δ 8.03 (1H, d, $J = 8.2$ Hz), 7.91 (1H, d, $J = 8.2$ Hz), 7.59 (1H, s), 7.55 (1H, d, $J = 1.4$ Hz), 7.52 (1H, dd, $J = 8.2$ and 1.4 Hz), 7.42 (1H, dd, $J = 3.7$ and 1.1 Hz), 7.34 (1H, d, $J = 5.2$ and 1.1 Hz), 7.31–7.33 (1H, m), 7.13 (1H, dd, $J = 5.2$ and 3.7 Hz), 4.35 (2H, q, $J = 7.2$ Hz), 1.47 (3H, t, $J = 7.2$ Hz); $^{13}\text{C NMR}$ (125 MHz, CDCl_3): δ 145.4, 141.4, 140.6, 132.6, 128.2, 124.9, 123.3, 122.3, 122.0, 121.83, 121.62, 120.9, 119.5, 118.2, 111.7, 106.0, 37.8, 13.9;

UV-vis (CH_2Cl_2): $\lambda_{\text{max}}^{\text{abs}}$ (relative intensity) 267 (0.935), 332 (1.00) nm; MALDI-TOF-MS (Dith, positive): m/z 354.59 (M^+). Elemental analysis calcd (%) for $\text{C}_{18}\text{H}_{14}\text{BrNS}\cdot 0.04\text{CHCl}_3$: C, 60.01; H, 3.92; N, 3.88%. Found: C, 59.92; H, 4.03; N, 3.83%.

Preparation of 5. Compound 17 (0.19 g, 0.536 mmol) was allowed to react with 13 (60 mg, 0.178 mmol) in the presence of K_2CO_3 (0.15 g, 1.07 mmol) and $[\text{Pd}(\text{PPh}_3)_4]$ (12 mg, 10.7 μmol) for 15 h according to the general Suzuki–Miyaura cross-coupling procedure. The crude material was purified by column chromatography (SiO_2 , toluene/hexane = 1:1) to give 5 (38 mg, 33%) as yellow solids. Mp 275 °C (Decomp.); ^1H NMR (300 MHz, CDCl_3): δ 8.08 (2H, d, J = 8.3 Hz), 8.07 (2H, d, J = 7.5 Hz), 7.66 (2H, s), 7.61 (2H, s), 7.59 (2H, d, J = 8.3 Hz), 7.53 (2H, d, J = 7.5 Hz), 7.46 (2H, s), 7.43 (2H, dd, J = 3.6 and 1.1 Hz), 7.32 (2H, dd, J = 5.1 and 1.1 Hz), 7.14 (2H, dd, J = 5.1 and 3.6 Hz), 4.47 (4H, q, J = 6.9 Hz), 1.53 (6H, t, J = 6.9 Hz); ^{13}C NMR (150 MHz, CDCl_3): δ 145.7, 144.6, 141.1, 132.38, 132.33, 128.2, 124.7, 124.2, 123.2, 122.4, 120.93, 120.88, 118.0, 117.6, 105.9, 105.5, 37.7, 14.1 (2 signals were missing); UV-vis (CH_2Cl_2): $\lambda_{\text{max}}^{\text{abs}}$ (ϵ) 269 (66 600), 401 (73 400) nm; HR-FAB-MS (NBA, Positive): m/z calcd for $\text{C}_{40}\text{H}_{30}\text{N}_2\text{S}_3^+$ 634.1571, found 634.1581 (M^+).

Preparation of 18. Compound 15 (0.40 g, 1.13 mmol) was allowed to react with 16 (0.18 mg, 0.871 mmol) in the presence of K_2CO_3 (0.24 mg, 1.74 mmol) and $[\text{Pd}(\text{PPh}_3)_4]$ (30 mg, 26.1 μmol) for 16 h according to the general Suzuki–Miyaura cross-coupling procedure. The crude material was purified by column chromatography (SiO_2 , toluene/hexane = 1:5) to give 18 (0.16 g, 51%) as pale yellow solids. Mp 136–137 °C; ^1H NMR (600 MHz, CDCl_3): δ 8.24 (1H, d, J = 1.8 Hz), 8.23 (1H, d, J = 1.9 Hz), 7.74 (1H, dd, J = 8.5 and 1.8 Hz), 7.55 (1H, dd, J = 8.6 and 1.9 Hz), 7.36 (1H, d, J = 8.5 Hz), 7.34 (1H, dd, J = 3.5 and 1.1 Hz), 7.28 (1H, dd, J = 5.1 and 1.1 Hz), 7.26 (1H, d, J = 8.6 Hz), 7.12 (1H, dd, J = 5.1 and 3.5 Hz), 4.30 (2H, q, J = 7.2 Hz), 1.41 (3H, t, J = 7.2 Hz); ^{13}C NMR (125 MHz, CDCl_3): δ 145.5, 139.7, 139.0, 128.7, 128.1, 126.2, 125.0, 124.6, 123.9, 123.4, 122.4, 122.2, 118.1, 111.9, 110.1, 109.1, 37.8, 13.9; UV-vis (CH_2Cl_2): $\lambda_{\text{max}}^{\text{abs}}$ 304 nm; MALDI-TOF-MS (Dith, positive): m/z 356.57 [($\text{M} + \text{H}$) $^+$]. Elemental analysis calcd (%) for $\text{C}_{18}\text{H}_{14}\text{BrNS}$: C, 60.68; H, 3.96; N, 3.93%. Found: C, 60.51; H, 3.95; N, 3.94%.

Preparation of 6. Compound 18 (0.10 g, 0.281 mmol) was allowed to react with 13 (31 mg, 93.6 μmol) in the presence of K_2CO_3 (77 mg, 0.561 mmol) and $[\text{Pd}(\text{PPh}_3)_4]$ (6 mg, 5.6 μmol) for 15 h according to the general Suzuki–Miyaura cross-coupling procedure. The crude material was purified by column chromatography (SiO_2 , toluene/hexane = 1:1) to give 6 (14 mg, 24%) as yellow solids. Mp 274 °C (Decomp.); ^1H NMR (300 MHz, CDCl_3): δ 8.42 (2H, d, J = 1.5 Hz), 8.39 (2H, d, J = 1.6 Hz), 7.82 (2H, dd, J = 8.4 and 1.5 Hz), 7.77 (2H, dd, J = 8.4 and 1.6 Hz), 7.44 (2H, d, J = 8.4 Hz), 7.42 (2H, d, J = 8.4 Hz), 7.39 (2H, s), 7.37–7.39 (2H, m), 7.28 (2H, d, J = 5.4 Hz), 7.14 (2H, dd, J = 5.4 and 3.6 Hz), 4.40 (4H, q, J = 7.2 Hz), 1.49 (6H, t, J = 7.2 Hz); ^{13}C NMR (150 MHz, CDCl_3): δ 145.8, 143.8, 140.06, 139.97, 128.1, 126.2, 126.1, 124.7, 124.3, 123.8, 123.5, 123.1, 122.2, 118.2, 117.7, 109.12, 109.09, 37.9, 14.0 (1 signal was missing); UV-vis (CH_2Cl_2): $\lambda_{\text{max}}^{\text{abs}}$ (ϵ) 315 (47 700), 362 (37 100) nm; MALDI-TOF-MS (Dith, positive): m/z 634.17 [($\text{M} + \text{H}$) $^+$]. Elemental analysis calcd (%) for $\text{C}_{40}\text{H}_{30}\text{N}_2\text{S}_3\cdot 0.13\text{CHCl}_3$: C, 74.11; H, 4.67; N, 4.31%. Found: C, 74.15; H, 4.96; N, 4.41%.

Preparation of 20. An *n*-BuLi hexane solution (2.64 M, 0.73 mL, 1.19 mmol) was added dropwise to a solution of 14 (0.20 mg, 0.566 mmol) in dry THF (20 mL) at -98 °C under an argon atmosphere. After the mixture was stirred at -98 °C for 1.5 h, trimethoxyborane (0.15 mL, 1.36 mmol) was added dropwise to the mixture. The resulting mixture was stirred at room temperature for 18 h. After the reaction was quenched by adding aqueous HCl (3 M, 40 mL), the organic phase was separated, and the aqueous phase was extracted with EtOAc (10 mL \times 6). The combined organic phase was washed with water (10 mL \times 3), dried over anhydrous MgSO_4 , and concentrated under reduced pressure to give crude diboronic acid 19 (0.14 g) as a white solid. A mixture of the crude 19 (0.14 g) and anhydrous pinacol (0.17 g, 1.45 mmol) in THF (25 mL) was heated at the refluxing temperature for 20 h. The mixture was concentrated under reduced

pressure. After the residue was dissolved into CHCl_3 (20 mL) and water (20 mL), the organic phase was separated, and the aqueous phase was extracted with CHCl_3 (5 mL \times 5). The combined organic phase was washed with water (5 mL \times 3), dried over anhydrous MgSO_4 , and concentrated under reduced pressure. The residue was purified by column chromatography (SiO_2 , toluene) to give 20 (45 mg, 18%) as white solids. An analytically pure material was obtained by recycling GPC eluting with CHCl_3 . Mp 280 °C; ^1H NMR (300 MHz, CDCl_3): δ 8.13 (2H, d, J = 7.8 Hz), 7.90 (2H, s), 7.68 (2H, d, J = 7.8 Hz), 4.47 (2H, q, J = 7.0 Hz), 1.46 (3H, t, J = 7.0 Hz), 1.41 (24H, s); ^{13}C NMR (75 MHz, CDCl_3): δ 140.0, 125.2, 124.9, 120.2, 115.1, 83.9, 37.5, 25.0, 14.4 (1 signal was missing); MALDI-TOF-MS (Dith, positive): m/z 447.76 (M^+). Anal. Calcd for $\text{C}_{26}\text{H}_{35}\text{B}_2\text{NO}_4\cdot 0.12\text{CHCl}_3$ (461.51): C, 67.98; H, 7.67; N, 3.03%. Found: C, 67.97; H, 7.61; N, 3.14%.

Preparation of 24. 2,5-Dibromothiophene (23) (42 μL , 0.374 mmol) was allowed to react with 22 (40 mg, 0.124 mmol) in the presence of K_2CO_3 (52 mg, 0.374 mmol) and $[\text{Pd}(\text{PPh}_3)_4]$ (4 mg, 3.7 μmol) for 6 h according to the general Suzuki–Miyaura cross-coupling procedure. The crude material was purified by column chromatography (SiO_2 , toluene/hexane = 1:10) to give 24 (9 mg, 20%) as pale yellow solids. Mp 107–109 °C; ^1H NMR (300 MHz, CDCl_3): δ 8.08 (1H, d, J = 7.9 Hz), 8.07 (1H, d, J = 8.0 Hz), 7.50 (1H, s), 7.47 (1H, d, J = 8.0 Hz), 7.41 (1H, d, J = 7.9 Hz), 7.40 (1H, d, J = 8.0 Hz), 7.23 (1H, d, J = 8.0 Hz), 7.16 (1H, d, J = 3.8 Hz), 7.07 (1H, d, J = 3.8 Hz), 4.40 (2H, q, J = 7.2 Hz), 1.47 (3H, t, J = 7.2 Hz); ^{13}C NMR (125 MHz, CDCl_3): δ 147.2, 140.3, 131.3, 131.0, 126.0, 123.2, 122.9, 122.7, 121.0, 120.6, 119.3, 117.2, 111.0, 108.6, 105.5, 37.7, 13.9 (1 signal was missing); UV-vis (CH_2Cl_2): $\lambda_{\text{max}}^{\text{abs}}$ (relative intensity) 330 (1.00), 267 (0.97) nm; HR-FAB-MS (NBA, positive): m/z calcd for $\text{C}_{18}\text{H}_{14}\text{BrNS}^+$ 357.0010, found 357.0009 (M^+).

Preparation of 7. Compound 24 (20 mg, 56.1 μmol) was allowed to react with 20 (11 mg, 25.5 μmol) in the presence of K_2CO_3 (14 mg, 0.102 mmol) and $[\text{Pd}(\text{PPh}_3)_4]$ (2 mg, 1.5 μmol) for 9 h according to the general Suzuki–Miyaura cross-coupling procedure. The crude material was purified by column chromatography (SiO_2 , CHCl_3 /hexane = 1:1) to give 7 (12 mg, 63%) as yellow solids. Mp 295 °C (Decomp.); ^1H NMR (50 °C, 600 MHz, CDCl_3): δ 8.11 (2H, d, J = 8.2 Hz), 8.10 (2H, d, J = 7.3 Hz), 8.09 (2H, d, J = 8.0 Hz), 7.67 (4H, s), 7.59 (2H, d, J = 8.2 Hz), 7.58 (2H, d, J = 8.0 Hz), 7.41–7.49 (8H, m), 7.22–7.27 (2H, m), 4.44–4.52 (6H, m), 1.49–1.52 (9H, m); ^{13}C NMR (50 °C, 150 MHz, CDCl_3): δ 145.0, 144.8, 141.3, 140.9, 140.7, 132.59, 132.40, 125.9, 124.26, 124.22, 123.1, 122.87, 122.70, 120.93, 120.5, 119.3, 117.8, 117.5, 108.7, 105.6, 37.8, 37.8, 14.1, 14.0 (1 signal was missing); UV-vis (CH_2Cl_2): $\lambda_{\text{max}}^{\text{abs}}$ (ϵ) 407 (75 200), 325 (19 600), 265 (57 800) nm; HR-FAB-MS (NBA, positive): m/z calcd for $\text{C}_{50}\text{H}_{39}\text{N}_3\text{S}_2^+$ 745.2585, found 745.2603 (M^+).

Preparation of 25. To a solution of 2 (0.20 g, 0.556 mmol) in DMF (20 mL) was added dropwise *N*-bromosuccinimide (0.20 g, 1.11 mmol) in DMF (20 mL) under light protection, and the resulting mixture was stirred for 2 h at room temperature. After the reaction was quenched by adding water (100 mL), the organic phase was separated, and the aqueous phase was extracted with toluene/EtOAc (1:1, 5 mL \times 4). The combined organic phase was washed with water (5 mL \times 3), dried over anhydrous MgSO_4 , and concentrated under reduced pressure. The residue was purified by column chromatography (SiO_2 , toluene/hexane = 1:3) to give 26 (0.28 g, 96%) as pale yellow solids. Mp 172–174 °C; ^1H NMR (300 MHz, CDCl_3): δ 8.24 (2H, d, J = 1.8 Hz), 7.66 (2H, dd, J = 8.5 and 1.8 Hz), 7.41 (2H, d, J = 8.5 Hz), 7.06–7.11 (4H, m), 4.38 (2H, q, J = 7.2 Hz), 1.47 (3H, t, J = 7.2 Hz); ^{13}C NMR (125 MHz, CDCl_3): δ 147.1, 140.1, 130.9, 125.4, 124.4, 123.3, 122.3, 117.9, 110.1, 109.2, 37.9, 14.0; UV-vis (CH_2Cl_2): $\lambda_{\text{max}}^{\text{abs}}$ (relative intensity) 317 (1.00), 269 (0.58), 256 (0.55) nm; MALDI-TOF-MS (Dith, positive): m/z 518.37 [($\text{M} + \text{H}$) $^+$]. Elemental analysis calcd (%) for $\text{C}_{22}\text{H}_{15}\text{Br}_2\text{NS}_2$: C, 51.08; H, 2.92; N, 2.71%. Found: C, 51.29; H, 3.03; N, 2.69%.

Preparation of 8. Compound 25 (27 mg, 51.9 μmol) was allowed to react with 26 (50 mg, 0.156 mmol) in the presence of K_2CO_3 (24 mg, 0.171 mmol) and $[\text{Pd}(\text{PPh}_3)_4]$ (4 mg, 3.1 μmol) for 20 h according to the general Suzuki–Miyaura cross-coupling procedure.

The crude material was purified by column chromatography (SiO₂, toluene/hexane = 1:1) to give **8** (25 mg, 64%) as yellow solids. Mp 290 °C (Decomp.); ¹H NMR (500 MHz, CDCl₃): δ 8.43 (2H, s), 8.40 (2H, s), 8.18 (2H, d, *J* = 7.6 Hz), 7.81 (4H, d, *J* = 8.0 Hz), 7.50 (2H, t, *J* = 7.6 Hz), 7.43 (4H, d, *J* = 8.0 Hz), 7.42–7.44 (2H, m), 7.37–7.41 (4H, m), 7.28 (2H, t, *J* = 7.6 Hz), 4.39 (6H, q, *J* = 6.8 Hz), 1.47 (9H, t, *J* = 6.8 Hz); ¹³C NMR (150 MHz, CDCl₃): δ 144.0, 143.7, 140.5, 139.9, 139.5, 126.3, 126.08, 126.01, 124.3, 124.0, 123.56, 123.54, 120.7, 123.09, 123.03, 119.1, 117.79, 117.68, 109.1, 108.90, 108.79, 37.8, 14.0 (3 signals were missing); UV–vis (CH₂Cl₂): λ_{max}^{abs} (ε) 380 (sh, 56 300), 349 (64 600), 314 (42 500) nm; MALDI-TOF-MS (Dith, positive): *m/z* 745.28 (M⁺). Elemental analysis calcd (%) for C₅₀H₃₉N₃S₂·0.24CHCl₃: C, 77.89; H, 5.10; N, 5.42%. Found: C, 77.74; H, 5.61; N, 5.24%.

Preparation of 28. Compound **27** (1.90 g, 4.76 mmol) was allowed to react with **16** (0.50 g, 2.38 mmol) in the presence of K₂CO₃ (0.66 g, 4.76 mmol) and [Pd(PPh₃)₄] (55 mg, 45.6 μmol) for 13 h according to the general Suzuki–Miyaura cross-coupling procedure. The crude material was purified by column chromatography (SiO₂, toluene/hexane = 1:10) to afford **28** (0.62 g, 63%) as white solids. Mp 118–119 °C; ¹H NMR (300 MHz, CDCl₃): δ 8.02 (1H, d, *J* = 8.1 Hz), 7.80 (1H, d, *J* = 8.2 Hz), 7.74 (1H, s), 7.57 (1H, s), 7.51 (1H, d, *J* = 8.1 Hz), 7.51 (1H, d, *J* = 8.2 Hz), 7.41 (1H, dd, *J* = 4.9 and 3.5 Hz), 7.32 (1H, d, *J* = 4.9 Hz), 7.13 (1H, dd, *J* = 4.9 and 3.5 Hz), 4.26 (2H, t, *J* = 7.2 Hz), 1.88 (2H, tt, *J* = 7.2 and 7.2 Hz), 1.23–1.48 (6H, m), 0.89 (3H, t, *J* = 6.7 Hz); ¹³C NMR (75 MHz, CDCl₃): δ 145.4, 141.7, 140.9, 132.4, 128.1, 124.7, 123.2, 122.1, 121.77, 121.60, 121.41, 120.7, 119.3, 118.0, 111.7, 106.0, 43.1, 31.5, 28.8, 26.9, 22.6, 14.1; UV–vis (CH₂Cl₂): λ_{max}^{abs} (relative intensity) 355 (sh, 0.54), 332 (0.93), 267 (1.00) nm; HR-FAB-MS (NBA, positive): *m/z* calcd for C₂₂H₂₂BrNS⁺ 413.0636, found 413.0645 (M⁺).

Preparation of 29. A mixture of **28** (38 mg, 0.091 mmol), CuI (176 mg, 0.091 mmol), and LiI (122 mg, 0.091 mmol) in DMSO (4 mL) was stirred at 150 °C for 24 h. The reaction was quenched by adding aqueous NaHSO₃ (10 mL). The organic phase was separated, and the aqueous phase was extracted with toluene/EtOAc (1:1, 10 mL × 4). The combined organic phase was washed with water (20 mL × 3), dried over anhydrous MgSO₄, and concentrated under reduced pressure to afford **29** (40 mg) as white solids, which contains ca. 10% of **28** as an inseparable material. The crude **29** was used in the next reaction without further purification. Mp 120–122 °C; ¹H NMR (300 MHz, CDCl₃): δ 8.02 (1H, d, *J* = 8.1 Hz), 7.91 (1H, d, *J* = 8.2 Hz), 7.58 (1H, s), 7.54 (1H, s), 7.51 (1H, d, *J* = 8.1 Hz), 7.41 (1H, dd, *J* = 3.6 and 1.1 Hz), 7.33 (1H, d, *J* = 8.2 Hz), 7.32 (1H, dd, *J* = 5.1 and 1.1 Hz), 7.13 (1H, dd, *J* = 5.1 and 3.6 Hz), 4.27 (2H, t, *J* = 7.2 Hz), 1.89 (2H, tt, *J* = 7.2 and 7.2 Hz), 1.23–1.48 (6H, m), 0.89 (3H, t, *J* = 7.0 Hz); ¹³C NMR (75 MHz, CDCl₃): δ 145.4, 142.0, 140.7, 132.7, 128.2, 127.9, 124.8, 123.3, 122.2, 121.86, 121.79, 120.8, 118.1, 117.8, 106.1, 90.4, 43.2, 31.6, 28.9, 27.0, 22.6, 14.1; UV–vis (CH₂Cl₂): λ_{max}^{abs} (relative intensity) 360 (sh, 0.52), 334 (0.98), 267 (1.00) nm; MALDI-TOF-MS (Dith, positive): *m/z* 458.96 (M⁺).

Preparation of 31. Crude compound **29** (40 mg) was allowed to react with **30** (19 mg, 65.3 μmol) in the presence of K₂CO₃ (18 mg, 0.131 mmol) and [Pd(PPh₃)₄] (7 mg, 6.5 μmol) for 2 h according to the general Suzuki–Miyaura cross-coupling procedure. The crude material was purified by column chromatography (SiO₂, toluene/hexane = 1:10) to afford **31** (24 mg, 65% in 2 steps) as yellow solids. Mp 179–181 °C; ¹H NMR (300 MHz, CDCl₃): δ 8.05 (1H, d, *J* = 8.1 Hz), 8.04 (1H, d, *J* = 8.1 Hz), 7.59 (1H, d, *J* = 1.2 Hz), 7.51 (1H, dd, *J* = 8.1 and 1.2 Hz), 7.48 (1H, d, *J* = 1.5 Hz), 7.42 (1H, dd, *J* = 3.6 and 1.1 Hz), 7.40 (1H, dd, *J* = 8.1 and 1.5 Hz), 7.32 (1H, dd, *J* = 5.1 and 1.1 Hz), 7.15 (1H, d, *J* = 3.8 Hz), 7.13 (1H, dd, *J* = 5.1 and 3.6 Hz), 7.08 (1H, d, *J* = 3.8 Hz), 4.34 (2H, t, *J* = 7.2 Hz), 1.92 (2H, tt, *J* = 7.2 and 7.2 Hz), 1.23–1.48 (6H, m), 0.89 (3H, t, *J* = 7.0 Hz); ¹³C NMR (75 MHz, CDCl₃): δ 147.2, 145.6, 141.61, 141.46, 132.4, 131.4, 131.0, 128.2, 124.8, 123.2, 122.6, 122.1, 120.91, 120.86, 118.0, 117.4, 111.1, 106.1, 105.8, 43.2, 31.6, 29.0, 27.0, 22.7, 14.2 (1 signal was missing); UV–vis (CH₂Cl₂): λ_{max}^{abs} (relative intensity) 380 (sh, 0.72), 357 (1.00), 270 (0.85) nm; MALDI-TOF-MS (Dith, positive): *m/z* 492.92

(M⁺). Elemental analysis calcd (%) for C₂₆H₂₄BrNS₂·0.09CHCl₃: C, 62.02; H, 4.80; N, 2.77%. Found: C, 62.05; H, 4.84; N, 2.78%.

Preparation of 9. Compound **31** (50 mg, 0.101 mmol) was allowed to react with **32** (23 mg, 46.0 μmol) in the presence of K₂CO₃ (32 mg, 0.230 mmol) and [Pd(PPh₃)₄] (3 mg, 2.7 μmol) for 1 h according to the general Suzuki–Miyaura cross-coupling procedure. The yellow precipitate was collected by filtration and successively washed with EtOAc (10 mL) and CH₂Cl₂ (5 mL) and recrystallized from CHCl₃/hexane twice to afford **9** (12 mg, 24%) as yellow solids. Mp 269–271 °C; ¹H NMR (80 °C, 600 MHz, 1,1,2,2-tetrachloroethane-*d*₂): δ 8.13 (2H, d, *J* = 7.7 Hz), 8.11 (2H, d, *J* = 8.6 Hz), 8.10 (2H, d, *J* = 8.3 Hz), 7.71 (2H, s), 7.70 (2H, s), 7.66 (2H, s), 7.60–7.64 (4H, m), 7.56 (2H, d, *J* = 8.3 Hz), 7.46–7.52 (6H, m), 7.37 (2H, d, *J* = 4.3 Hz), 7.16–7.20 (2H, m), 4.45 (2H, t, *J* = 7.2 Hz), 4.42 (4H, t, *J* = 7.3 Hz), 2.05 (2H, tt, *J* = 7.2 and 7.2 Hz), 2.02 (4H, tt, *J* = 7.3 and 7.3 Hz), 1.37–1.62 (18H, m), 0.99 (3H, t, *J* = 7.3 Hz), 0.97 (6H, t, *J* = 7.1 Hz); ¹³C NMR (80 °C, 150 MHz, 1,1,2,2-tetrachloroethane-*d*₂): δ 145.6, 144.8, 141.77, 141.71, 132.42, 132.39, 132.36, 128.1, 124.7, 124.2, 123.7, 123.2, 122.45, 122.41, 122.38, 120.75, 120.70, 120.7, 120.4, 118.1, 117.85, 117.81, 106.2, 105.8, 43.3, 31.5, 29.0, 27.0, 22.5, 14.0 (5 signals ascribed to the aromatic groups were missing due to the low solubility, and 6 signals ascribed to the alkyl groups were overlapped); UV–vis (CH₂Cl₂): λ_{max}^{abs} (ε) 416 (81 200), 340 (sh, 24 400), 300 (sh, 19 200), 270 (65 500) nm; HR-FAB-MS (NBA, positive): *m/z* calcd for C₇₀H₆₈N₃S₄⁺ 1078.4296, found 1078.4314 [(M + H)⁺]. Elemental analysis calcd (%) for C₇₀H₆₇N₃S₄·0.43CHCl₃: C, 74.87; H, 6.01; N, 3.71%. Found: C, 74.88; H, 6.11; N, 3.90%.

Preparation of 34. To a solution of **33** (0.20 g, 0.481 mmol) in DMF (20 mL) was added dropwise *N*-bromosuccinimide (86 mg, 0.481 mmol) in DMF (20 mL) under light protection, and the resulting mixture was stirred for 4 h at room temperature. The reaction was quenched by adding water (100 mL). The organic phase was separated, and the aqueous phase was extracted with toluene/EtOAc (1:1, 10 mL × 4). The combined organic phase was washed with water (10 mL × 3), dried over anhydrous MgSO₄, and concentrated under reduced pressure. The residue was purified by column chromatography (SiO₂, toluene/hexane = 1:20) to afford **34** (0.13 g, 59%) as a yellow oil. An analytically pure material was obtained by recycling GPC eluting with CHCl₃. ¹H NMR (300 MHz, CDCl₃): δ 8.32 (1H, d, *J* = 1.7 Hz), 8.24 (1H, d, *J* = 1.8 Hz), 7.75 (1H, dd, *J* = 8.5 and 1.7 Hz), 7.63 (1H, dd, *J* = 8.4 and 1.8 Hz), 7.39 (1H, d, *J* = 8.5 Hz), 7.38 (1H, d, *J* = 8.4 Hz), 7.36 (1H, dd, *J* = 3.4 and 1.1 Hz), 7.27 (1H, dd, *J* = 5.3 and 1.1 Hz), 7.12 (1H, dd, *J* = 5.3 and 3.4 Hz), 7.09 (1H, d, *J* = 3.8 Hz), 7.06 (1H, d, *J* = 3.8 Hz), 4.29 (2H, t, *J* = 7.2 Hz), 1.88 (2H, tt, *J* = 7.2 and 7.2 Hz), 1.24–1.44 (6H, m), 0.88 (3H, t, *J* = 6.4 Hz); ¹³C NMR (75 MHz, CDCl₃): δ 147.2, 145.6, 140.51, 140.38, 130.8, 128.1, 126.0, 125.0, 124.6, 124.0, 123.7, 123.2, 123.0, 122.1, 117.9, 117.6, 109.8, 109.27, 109.26, 43.2, 31.6, 29.0, 27.0, 22.6, 14.1 (1 signal was missing); UV–vis (CH₂Cl₂): λ_{max}^{abs} (relative intensity) 345 (sh, 0.59), 316 (1.00), 268 (0.66), 256 (0.61) nm; MALDI-TOF-MS (Dith, positive): *m/z* 494.03 [(M+H)⁺]. Elemental analysis calcd (%) for C₂₆H₂₄BrNS₂·0.07CHCl₃: C, 62.27; H, 4.82; N, 2.78%. Found: C, 62.28; H, 4.75; N, 2.77%.

Preparation of 10. Compound **34** (0.10 g, 0.202 mmol) was allowed to react with **35** (37 mg, 91.9 μmol) in the presence of K₂CO₃ (63 mg, 0.460 mmol) and [Pd(PPh₃)₄] (6 mg, 5.5 μmol) for 18 h according to the general Suzuki–Miyaura cross-coupling procedure. The crude material was purified by column chromatography (SiO₂, toluene/hexane = 1:2) to afford **10** (23 mg, 23%) as yellow solids. Mp 290 °C (Decomp.); ¹H NMR (300 MHz, CDCl₃): δ 8.43 (2H, s), 8.42 (2H, s), 8.38 (2H, d, *J* = 1.6 Hz), 7.81 (4H, dd, *J* = 8.6 and 1.5 Hz), 7.75 (2H, dd, *J* = 8.5 and 1.6 Hz), 7.42 (2H, d, *J* = 8.6 Hz), 7.38–7.41 (8H, m), 7.37 (2H, dd, *J* = 3.6 and 1.1 Hz), 7.26 (2H, dd, *J* = 4.7 and 1.1 Hz), 7.11 (2H, dd, *J* = 4.7 and 3.6 Hz), 4.31 (6H, t, *J* = 7.2 Hz), 1.91 (6H, tt, *J* = 7.2 and 7.2 Hz), 1.26–1.46 (18H, m), 0.85–0.93 (9H, m); ¹³C NMR (150 MHz, CDCl₃): δ 145.8, 143.81, 143.73, 140.50, 140.39, 128.1, 126.20, 126.15, 125.9, 124.6, 124.25, 124.19, 123.7, 123.38, 123.36, 123.34, 123.06, 123.03, 122.1, 118.0, 117.5, 109.29, 109.26, 43.4, 31.7, 29.1, 27.1, 22.7, 14.2 (9 signals were missing); UV–vis (CH₂Cl₂): λ_{max}^{abs} (ε) 380 (sh, 58 500), 358 (65 400), 321 (67 200)

nm; MALDI-TOF-MS (Dith, positive): m/z 1078.34 [(M + H)⁺]. Elemental analysis calcd (%) for C₇₀H₆₇N₃S₄·0.13CHCl₃: C, 76.99; H, 6.18; N, 3.84%. Found: C, 76.97; H, 6.26; N, 3.80%.

■ ASSOCIATED CONTENT

■ Supporting Information

General experimental methods, X-ray data including a cif file, fluorescence lifetime data, electrochemical data, theoretical data, and ¹H and ¹³C NMR spectra of all new compounds. This material is available free of charge via the Internet at <http://pubs.acs.org>.

■ AUTHOR INFORMATION

Corresponding Author

*E-mail: nakamura@gunma-u.ac.jp.

Notes

The authors declare no competing financial interest.

■ ACKNOWLEDGMENTS

This work was financially supported by Grants-in-Aid for Scientific Research from MEXT, Japan (No. 24550040). The authors thank Prof. Soichiro Kyushin (Gunma University) for generous permission to use an X-ray diffractometer.

■ REFERENCES

- (1) (a) *Organic Electronics: Materials, Manufacturing and Applications*; Klauk, H., Eds.; Wiley-VCH: Weinheim, 2006. (b) *Organic Light Emitting Devices: Synthesis, Properties and Applications*; Müllen, K., Scherf, U., Eds.; Wiley-VCH: Weinheim, 2006. (c) *Functional Organic Materials*; Müller, T. J. J., Bunz, U. H. F., Eds.; Wiley-VCH: Weinheim, 2007. (d) *Organic Electroluminescence*; Kakafi, Z. H., Eds.; CRC Press: New York, 2005. (e) *Carbon-Rich Compounds: From Molecules to Materials*; Haley, M. M., Tykwinski, R. R., Eds.; Wiley-VCH: Weinheim, 2006.
- (2) (a) Kelley, T. W.; Baude, P. F.; Gerlach, C.; Ender, D. E.; Mures, D.; Haase, M. A.; Vogel, D. E.; Theiss, S. D. *Chem. Mater.* **2004**, *16*, 4413. (b) Special issue on Organic Electronics and Optoelectronics: Forrest, S. R., Thompson, M. E., Eds. *Chem. Rev.* **2007**, *107*, 923. (c) Bendikov, M.; Wudl, F.; Perepichka, D. F. *Chem. Rev.* **2004**, *104*, 4891. (d) Shirota, Y.; Kageyama, H. *Chem. Rev.* **2007**, *107*, 953. (e) Wu, W.; Liu, Y.; Zhu, D. *Chem. Soc. Rev.* **2010**, *39*, 1489.
- (3) *Electronic Materials: The Oligomer Approach*; Müllen, K., Wegner, C., Eds.; Wiley-VCH: Weinheim, 1998.
- (4) (a) Martin, R. E.; Diederich, F. *Angew. Chem., Int. Ed.* **1999**, *38*, 1350. (b) Gierschner, J.; Cornil, J.; Egelhaaf, H.-J. *Adv. Mater.* **2007**, *19*, 173.
- (5) (a) Tao, N. J. *Nat. Nanotechnol.* **2006**, *1*, 173. (b) Cuevas, J. C.; Scheer, E. *Molecular Electronics: An Introduction to Theory and Experiment*; World Scientific: Singapore, 2010.
- (6) For reviews, see: (a) Gražulevičius, J. V.; Strohhriegl, P.; Pielichowski, J.; Pielichowski, K. *Prog. Polym. Sci.* **2003**, *28*, 1297. (b) Morin, J.-F.; Leclerc, M.; Adès, D.; Siove, A. *Macromol. Rapid Commun.* **2005**, *26*, 761. (c) Blouin, N.; Leclerc, M. *Acc. Chem. Res.* **2008**, *41*, 1110. (d) Boudreault, P.-L. T.; Morin, J.-F.; Leclerc, M. In *Design and Synthesis of Conjugated Polymers*; Leclerc, M., Morin, J.-F., Eds.; Wiley-VCH: Weinheim, 2010; p 205.
- (7) The recent development of carbazole-based π -functional materials is summarized in ref 8.
- (8) (a) Kato, S.-i.; Shimizu, S.; Taguchi, H.; Kobayashi, A.; Tobita, S.; Nakamura, Y. *J. Org. Chem.* **2012**, *77*, 3222. (b) Kato, S.-i.; Noguchi, H.; Kobayashi, A.; Yoshihara, T.; Tobita, S.; Nakamura, Y. *J. Org. Chem.* **2012**, *77*, 9120.
- (9) (a) Michinobu, T.; Osako, H.; Shigehara, K. *Macromol. Rapid Commun.* **2008**, *29*, 111. (b) Michinobu, T.; Osako, H.; Shigehara, K. *Macromolecules* **2009**, *42*, 8172. (c) Michinobu, T.; Osako, H.; Murata, K.; Shigehara, K. *Chem. Lett.* **2010**, *39*, 168.
- (10) Dierschke, F.; Grimsdale, A. C.; Müllen, K. *Synthesis* **2003**, 2470.
- (11) (a) Mishra, A.; Ma, C.-Q.; Bäuerle, P. *Chem. Rev.* **2009**, *109*, 1141. (b) *Handbook of Thiophene-based Materials*; Perepichka, I. F., Perepichka, D. F., Eds.; Wiley-VCH: Weinheim, 2009.
- (12) For selected examples, see: (a) Morin, J.-F.; Drolet, N.; Tao, Y.; Leclerc, M. *Chem. Mater.* **2004**, *16*, 4619. (b) Belletête, B.; Morin, J.-F.; Leclerc, M.; Durocher, J. *Phys. Chem. A* **2005**, *109*, 6953. (c) Lu, J.; Xia, P. F.; Lo, P. K.; Tao, Y.; Wong, M. S. *Chem. Mater.* **2006**, *18*, 6194. (d) Melucci, M.; Favaretto, L.; Bettini, C.; Gazzano, M.; Camaioni, N.; Maccagnani, P.; Ostojica, P.; Monari, M.; Barbarella, G. *Chem.—Eur. J.* **2007**, *13*, 10046. (e) Khanasa, T.; Praachumrak, N.; Rattanawan, R.; Jungstittiwong, S.; Keawin, T.; Sudyoadsuk, T.; Tuntulani, T.; Promarak, V. *J. Org. Chem.* **2013**, *78*, 6702. (f) Masuda, K.; Maeda, C. *Chem.—Eur. J.* **2013**, *19*, 2971.
- (13) Koumura, N.; Wang, Z.-S.; Mori, S.; Miyashita, M.; Suzuki, E.; Hara, K. *J. Am. Chem. Soc.* **2006**, *128*, 14256.
- (14) For selected examples of dye-sensitized solar cells, see: (a) Wang, Z.-S.; Koumura, N.; Cui, Y.; Takahashi, M.; Sekiguchi, H.; Mori, A.; Kubo, T.; Furube, A.; Hara, K. *Chem. Mater.* **2008**, *20*, 3993. (b) Koumura, N.; Wang, Z.-S.; Miyashita, M.; Uemura, Y.; Sekiguchi, H.; Cui, Y.; Mori, A.; Mori, S.; Hara, K. *J. Mater. Chem.* **2009**, *19*, 4829. (c) Ooyama, Y.; Shimada, Y.; Inoue, S.; Nagano, T.; Fujikawa, Y.; Komaguchi, K.; Imae, I.; Harima, Y. *New J. Chem.* **2011**, *35*, 111. (d) Lee, W.; Cho, N.; Kwon, J.; Ko, J.; Hong, J.-I. *Chem.—Asian J.* **2012**, *7*, 343. (e) Chen, C.; Liao, J.-Y.; Chi, Z.; Xu, B.; Zhang, X.; Kuang, D.-B.; Zhang, Y.; Liu, S.; Xu, J. *J. Mater. Chem.* **2012**, *22*, 8994. (f) Sudyoadsuk, T.; Pansay, S.; Morada, S.; Rattanawan, R.; Namuangruk, S.; Kaewin, T.; Jungstittiwong, S.; Promarak, V. *J. Org. Chem.* **2013**, 5051. See also a review: (g) Koumura, N.; Hara, K. *Heterocycles* **2013**, *87*, 275.
- (15) Some of the 3,6-linked oligomers were reported in a patent: Qiu, Y.; Li, Y.; Dong, H.; Wang, C. CN 101205227 A 20080625, 2008 (Tsinghua Univ., Beijing Visionox Technology Co., Ltd., Kunshan Visionox Company).
- (16) (a) Miyaura, N.; Yanagi, T.; Suzuki, A. *Synth. Commun.* **1981**, *11*, 513. (b) Miyaura, N.; Suzuki, A. *Chem. Rev.* **1995**, *95*, 2457.
- (17) In contrast to the previously reported thienylcarbazole systems,^{8a} the rotational disorder for the thiophene units is not observed in **6**.
- (18) All calculations were carried out using: Frisch, M. J.; Trucks, G. W.; Schlegel, H. B.; Scuseria, G. E.; Robb, M. A.; Cheeseman, J. R.; Scalmani, G.; Barone, V.; Mennucci, B.; Petersson, G. A.; Nakatsuji, H.; Caricato, M.; Li, X.; Hratchian, H. P.; Izmaylov, A. F.; Bloino, J.; Zheng, G.; Sonnenberg, J. L.; Hada, M.; Ehara, M.; Toyota, K.; Fukuda, R.; Hasegawa, J.; Ishida, M.; Nakajima, T.; Honda, Y.; Kitao, O.; Nakai, H.; Vreven, T.; Montgomery, Jr., J. A.; Peralta, J. E.; Ogliaro, F.; Bearpark, M.; Heyd, J. J.; Brothers, E.; Kudin, K. N.; Staroverov, V. N.; Keith, T.; Kobayashi, R.; Normand, J.; Raghavachari, K.; Rendell, A.; Burant, J. C.; Iyengar, S. S.; Tomasi, J.; Cossi, M.; Rega, N.; Millam, J. M.; Klene, M.; Knox, J. E.; Cross, J. B.; Bakken, V.; Adamo, C.; Jaramillo, J.; Gomperts, R.; Stratmann, R. E.; Yazyev, O.; Austin, A. J.; Cammi, R.; Pomelli, C.; Ochterski, J. W.; Martin, R. L.; Morokuma, K.; Zakrzewski, V. G.; Voth, G. A.; Salvador, P.; Dannenberg, J. J.; Dapprich, S.; Daniels, A. D.; Farkas, O.; Foresman, J. B.; Ortiz, J. V.; Cioslowski, J.; Fox, D. J. *Gaussian 09*, revision B.01; Gaussian, Inc.: Wallingford, CT, 2010.
- (19) For details in the structural optimization, see Figure S2 in the Supporting Information.
- (20) We cannot entirely rule out the possibility that the DFT calculations underestimate the planarity of **6**, because we examined only the B3LYP method for the calculations.
- (21) For the effective conjugation length of 3,6-functionalized carbazole derivatives, see: (a) Paliulis, O.; Ostrauskaite, J.; Gaidelis, V.; Jankauskas, V.; Strohhriegl, P. *Macromol. Chem. Phys.* **2003**, *204*, 1706. (b) Zhao, Z.; Xu, X.; Wang, H.; Lu, P.; Yu, G.; Liu, Y. *J. Org. Chem.* **2008**, *73*, S94.
- (22) No characteristic excimer fluorescence was observed.
- (23) The interpretation of the fluorescence spectra was kindly proposed by one of the referees.

(24) The emission decay profiles were numerically fitted by single exponential kinetics.

(25) (a) Chi, C.; Wegner, G. *Macromol. Rapid Commun.* **2005**, *26*, 1532. (b) Pommerehne, J.; Vestweber, H.; Guss, W.; Mahrt, R. F.; Bassler, H.; Porsch, M.; Daub, J. *Adv. Mater.* **1995**, *7*, 551.

(26) The quinoidal thiophene structure should contribute to the remarkably high electrochemical stability of the cationic species of **4**.

(27) We note that the optimized structures are strongly affected by the initial structures in general. We did not perform the conformation search for **1'**–**10'**.

(28) The oscillator strength for the HOMO–LUMO transition of **2'** is calculated to be only 0.006 at 341 nm, and the configuration interaction coefficient is 90%.